

TOWARDS FULL 4H-SiC BASED X-RAY BEAM MONITORING

M. Carulla† and M. Camarda, Paul Scherrer Institute, Villigen, Switzerland
 M. Birri, B. Meyer, D. Grolimund, C. Pradervand, O. S. Nida¹, A. Tsibizov¹, T. Ziemann¹,
 U. Grossner¹, Paul Scherrer Institute, Villigen, Switzerland
¹also at Advanced Power Semiconductor Laboratory, ETH Zurich, Switzerland

Abstract

In this work, we present a systematic theoretical and experimental investigation of the use of Silicon Carbide thin (thicknesses between 500 nm and 10 μm) low-doped large area ($>10\text{ mm}^2$) membranes as X-ray sensors for beam position monitoring (XBPM) applications at synchrotron light sources (SLS).

INTRODUCTION

SLS generates high brilliance ($>1\text{ kW/cm}^2$) coherent and polarized X-ray beam for e.g. diffraction experiments conducted at the different beamlines. Beam stability is a key issue to increase throughput and resolution, especially in the case of small ($<100\text{ nm}$ FWHM) beams [1]. This drove the demand for in-line, continuous, accurate and reliable monitoring. Semiconductor based X-ray Beam Position Monitors (XBPMs) are front to back quadrant detectors (Fig. 1) which provide continuous spatial and intensity information allowing, e.g. implementation of feedback loops to correct for example mirrors instabilities. Until recently, state-of-the-art commercial XBPMs were made of diamond, thanks to its excellent thermal conductivity, high melting point, wide bandgap and low absorption coefficient, i.e. high transparency (see Table 1) [2]. Diamond is not available as large single crystal wafers so the material availability and quality limit the sensor performance, thus the applications [3]. Nowadays, diamond XBPM are commercially available as small ($<25\text{ mm}^2$) single crystal or polycrystalline sensors [4, 5].

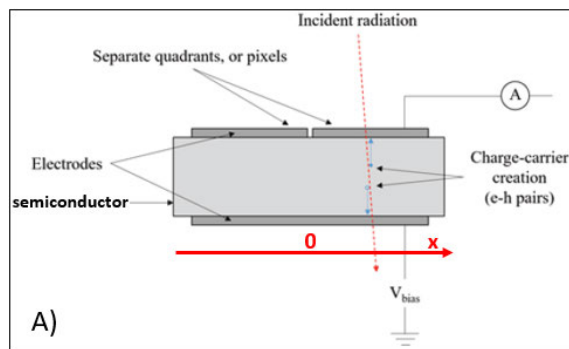


Figure 1: A schematic of a semiconductor based XBPM.

Table 1: Comparison of the Main Properties of Sc-Diamond and 4H-SiC

Property	Sc-Diamond	4H-SiC
Effective Quantum Yield per photon energy [1/eV]	0.077	0.128
X-ray attenuation length at 8keV [μm]	650	70
Thermal Conductivity [W/cmK]	22	4.9
Shottky Barrier Height (to nickel) [eV]	1.5	1.56

4H-SiC XBPM

Thanks to the mechanical and electrical properties of 4H-SiC (see Tab.1), as well as the 4H-SiC material maturity due to the power device industry, represents a superior alternative to diamond. However SiC was never tested for X-ray beam monitor application due to its high absorption coefficient (see Tab.1) and the thickness of the available substrates, i.e. $>350\text{ }\mu\text{m}$. In the last years, a newly developed/patented [2018P04211EP] doping selective electrochemical etching process makes possible the thinning of 4H-SiC substrates. 4H-SiC XBPM produced using doping selective electrochemical etching show superior optical (transparency) and electrical (dynamics, linearity and signal strength) properties in comparison to state-of-the-art commercial single crystal and polycrystalline diamond sensors, respectively [6].

Pink Beam and White Beam

Pink beam is the beam delimited by the region between the front-end and the monochromator, while whitebeam is the beam in the front-end region, just after the insertion device, as PSI beamline convention. The pink beam expected power is in the order of several hundred watts, so it is mandatory to have as-thin-as-possible XBPMs, to reduce the absorbed power and thus avoid thermal run-aways. Furthermore, a Rapid Thermal Annealing (RTA) of the XBPM metallization should be done, in order to form an alloy with silicon and so increase the evaporation temperature of the contacts.

In the other hand the expected power of white beam will be on the order of several thousand watts, for such applications a new XBPM design without membrane and a pinhole

† maria.carulla@psi.ch

Content from this work may be used under the terms of the CC BY 3.0 licence (© 2019). Any distribution of this work must maintain attribution to the author(s), title of the work, publisher, and DOI

in the centre of the detector has been realized, which will allow coping with the extreme intensives of the beams in front of the insertion devices.

DEVICE FABRICATION

4H-SiC XBPM were fabricated on 4 inches wafers with epitaxial layers grown on 375 μm in thickness $1 \times 10^{18} \text{ cm}^{-3}$ n-type nitrogen doped substrates. The epitaxial layers are either 2 or 10 μm in thickness $5 \times 10^{13} \text{ cm}^{-3}$ n-type nitrogen doped with a 0.5 μm thin $1 \times 10^{18} \text{ cm}^{-3}$ p-type layer aluminium doped on top (Fig. 2).

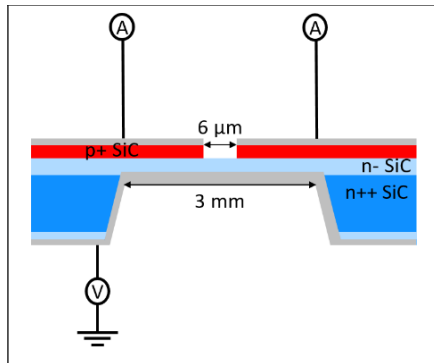


Figure 2: Cross section of the produced 4H-SiC XBPM devices.

The four-quadrant monitors were defined by means of reactive ion etching (RIE) in SF6 plasma, which etches the p-type layer using aluminium layer as a mask. The distance between quadrants is 6 μm . Then the area where the substrate was previously etched was defined by RIE of the low-doped n-type epitaxial layer on the backside using aluminium as a mask layer. The diameter of the circular opening is 3 mm. Afterwards, the front contacts are defined and the substrate is wet etched by means of the doping selective electrochemical etching which stops once it reach the membrane and the substrate is completely etched. Finally, 100 nm aluminium layer were deposited on the backside (Fig. 3). Up to 50 devices were produced per each wafer.

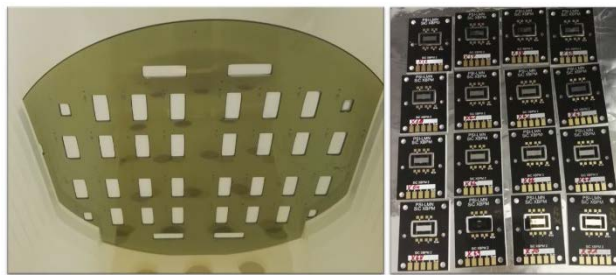


Figure 3: Picture of the produced XBP on wafer (left) and on PCB board (right).

MEASUREMENTS

First measurements of the produced XBPM devices were carried out on fully automated UV (325 nm) LED based screening system. 4H-SiC like other wide bandgap materials are not sensible to visible light, the energy of visible light is not enough to promote an electron from the valence band to the conduction band. On the other hand, UV-light does generate electron-hole pairs on the XBPM. Thus, the XBPM mounted on PCB board were tested with UV-light generated by a LED. Each XBPM was biased from the backside and the pads current was read by an ampere-meter. The current measurement of the illuminated BPM as a function of the reverse applied voltage for different devices from the same wafer shows a variation less than 10% (Fig. 4) showing the good stability of the process technology.

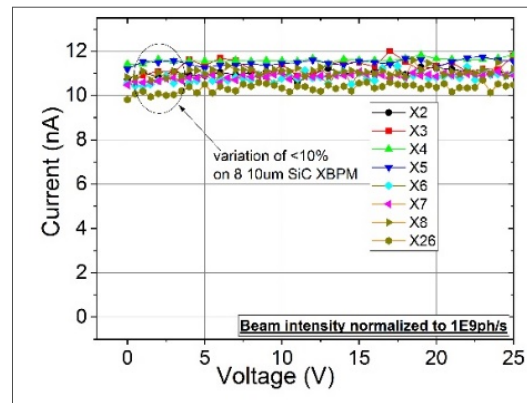


Figure 4: Current as a function of the reverse bias for different XBPM devices from the same wafer.

It is worth to notice that the XBPM devices can operate at 0 V thanks to the build-in voltage of the p-n junction, which depletes 9 μm and builds up an electric field in the junction which drift the generated e-h pairs [7].

PXI Beamline (Pink Beam)

After the first characterization on the UV-light setup, 2 μm thin XBPM device was installed on August 8th at the pink beam region of the SX06SA (PXI) beamline (Fig. 5. left). An RTA on the XBPM was performed before its installation on the beamline. An 80 μm diamond screen installed on the front-end *suppresses* beam energies lower than 2 keV. Although it does not *suppress* energies lower than 5.4 eV, i.e. visible light (Fig. 5, right).

The measured current on each pad is in the order of tens of μA , which is several order of magnitude lower than the expected one (1 A). Further simulation and experimental tests are currently underway to clarify the origin of this low measured.

Notwithstanding the low currents it was still possible align to the beam and calibrate the XBPM. The comparison of the current sum and storage ring current shows how the sum follows the top-up of the storage ring beam (Fig. 6).

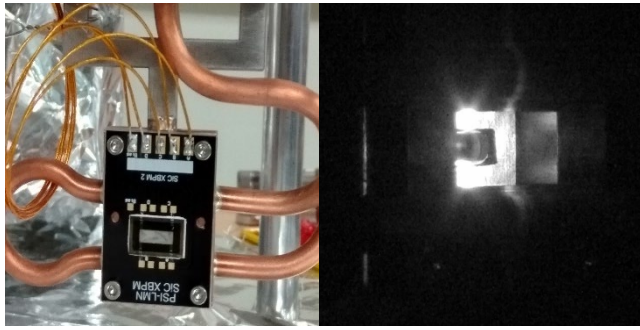


Figure 5: XBPM mounted on the copper stage for thermal dissipation (left). Picture taken during beam operation with a camera placed in one of the vacuum windows (right).

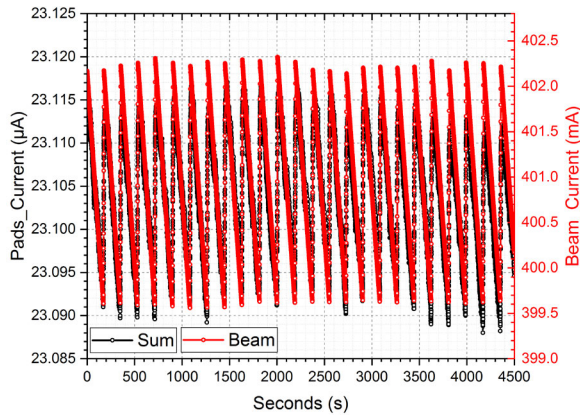


Figure 6: Sum of the 4 XBPM pads in black lines and storage ring beam current during one hour and a quarter.

After a month of operation, the XBPM keeps working showing the same current levels as the first day.

MicroSAX Beamline (After Monochromator)

MicroSAX beamline has a permanent two μm thin 4H-SiC XBPM, which was installed after the monochromator. The XBPM was not biased and the 4 pads were connected to a TetrAMM CAENels [8], which reads the 4 pads current simultaneously with a 24-bit resolution and 100 kHz sample rate. The data was recorded and processed by means of BEST system from CAENels.

The BPM orientation was set to 45° and the x and y beam positions were calculated using the Eq. (1) and (2), respectively.

$$X = K_X \frac{I_B + I_C - (I_A + I_D)}{(I_A + I_B + I_C + I_D)} + \text{offset}_X \quad (1)$$

$$Y = K_Y \frac{I_A + I_B - (I_C + I_D)}{(I_A + I_B + I_C + I_D)} + \text{offset}_Y \quad (2)$$

where IA, IB, IC and ID are the measured current on channel A, B, C and D, respectively. KX and KY were determined doing a scan in the x and y position.

A frequency analysis of the x and y position was performed. The data were acquired with a sample rate of 1000 Hz.

The FFT of the vertical and horizontal position acquired during the commissioning of a new $2 \mu\text{m}$ thin 4H-SiC XBPM at the microSAX beamline on September 2nd, showed a peak at 190 Hz (Fig. 7, top) before the shutdown of the machine. The same peak on this frequency was observed in another beamline. This peak at 190 Hz was introduced by the feedback system of the storage ring. After the feedback system was fixed, the peak at 190 Hz was suppressed (Fig. 7, bottom).

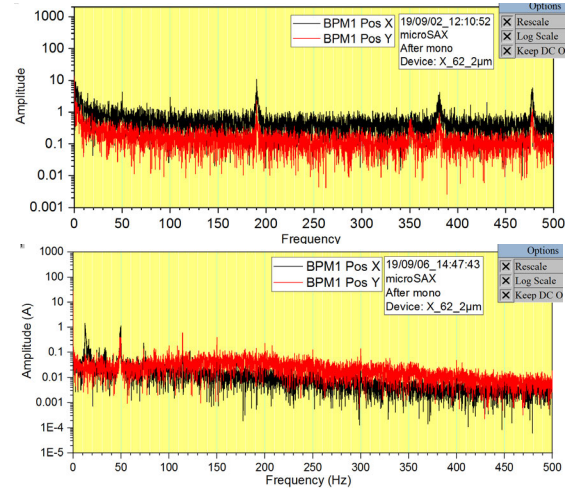


Figure 7: FFT of the X and Y position in black and red, respectively, before a machine shutdown due to storage ring instabilities (top) and after the feedback system of the storage ring was fixed (bottom).

Thanks to the implemented feedback schema, there is a factor 20 improvement on beam stability over energy scans (Fig. 8).

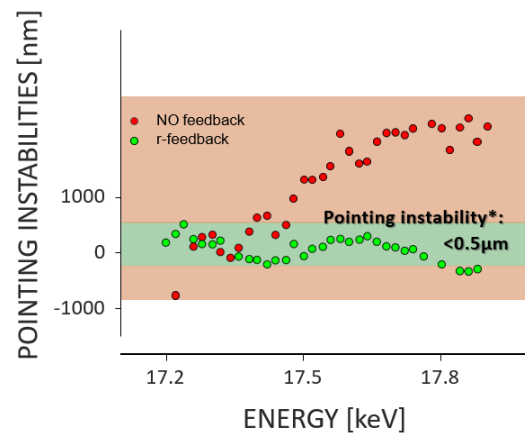


Figure 8: Energy scan over beam lateral instabilities before (red) and after (green) implementing the feedback schema.

CONCLUSION

4H-SiC XBPM have proven their transparency, linearity, signal strength dynamics compare to polycrystalline and single crystal diamond. Furthermore, 4H-SiC BPM can operate at 0 V.

The XBPM installed on the microSAX beamline fulfil with the expected resolution and temporal response, which allows the feedback and correction of the mirrors with a rate of 100 Hz.

Finally, the latest installation of 2 μm thin 4H-SiC XBPM in the pink beam region of the PXI beamline has fulfilled the expected reliabilities of thin SiC XBPMs, although more measurements and simulations have to be performed in order to understand the low current measured on the device.

REFERENCES

- [1] R. L. Owen, J. Juanhuix, and M. Fuchs, “Current advances in synchrotron radiation instrumentation for MX experiments,” *Arch. Biochem. Biophys.*, 2016. doi:10.1016/j.abb.2016.03.021
- [2] C. Schulze-Briese *et al.*, “A CVD-diamond based beam profile monitor for undulator radiation,” *Nucl. Instruments Methods Phys. Res. Sect. A Accel. Spectrometers, Detect. Assoc. Equip.*, vol. 467–468, pp. 230–234, Jul. 2001. doi:10.1016/S0168-9002(01)00281-9
- [3] K. Desjardins, M. Pomorski, J. Morse, and IUCr, “Ultra-thin optical grade scCVD diamond as X-ray beam position monitor,” *J. Synchrotron Radiat.*, vol. 21, no. 6, pp. 1217–1223, Nov. 2014. doi:10.1107/S1600577514016191
- [4] “CIVIDEC Instrumentation - CVD Diamond Technology applications.” <https://cividec.at/>
- [5] “Home - Dectris.” <https://www.dectris.com/>
- [6] S. Nida *et al.*, “Silicon carbide X-ray beam position monitors for synchrotron applications,” *J. Synchrotron Radiat.*, vol. 26, no. 1, pp. 28–35, Jan. 2019. doi:10.1107/S1600577518014248
- [7] B. Jayant Baliga, “Fundamentals of Power Semiconductor Devices.”
- [8] “TetrAMM - CAENels.” <https://www.caenels.com/products/tetramm/>